

## Self-Assembly of Shape Controlled Hierarchical Porous Thin Films: Mesopores and Nanoboxes

Luca Malfatti,<sup>†</sup> Paolo Falcaro,<sup>‡</sup> Daniela Marongiu,<sup>†</sup> Maria F. Casula,<sup>§</sup> Heinz Amenitsch,<sup>||</sup> and Plinio Innocenzi<sup>\*,†</sup>

<sup>†</sup>Laboratorio di Scienza dei Materiali e Nanotecnologie (LMNT), CR-INSTM, D.A.P.,  
Università di Sassari, Palazzo Pou Salid, Piazza Duomo 6, 07041 Alghero SS, Italy,

<sup>‡</sup>CSIRO Materials Science & Engineering, Gate 5 Normanby Road, Clayton VIC 3168, Australia,

<sup>§</sup>Dipartimento di Scienze Chimiche, Università di Cagliari, S.S. 554 bivio per Sestu, 09042 Monserrato CA, Italy, and <sup>||</sup>Institute of Biophysics and Nanosystems Research, Austrian Academy of Sciences, Schmiedlstrasse 6, 8042, Graz, Austria

Received May 20, 2009. Revised Manuscript Received August 11, 2009

Hierarchical porous thin films with well-defined pore dimensions and topologies have been obtained through an evaporation induced self-assembly process. The films show a cubic ordered array of mesopores together with the presence of well-defined nanoboxes that appear homogeneously dispersed in the material. The nanoboxes are formed by controlled crystallization of NaCl during the evaporation of the solvent when the film is deposited. The pores can be selectively emptied by thermal treatment and water washing allowing the preparation of a new generation of hierarchical porous materials.

### Introduction

Self-assembly of materials through evaporation of a solvent is a versatile route to obtain different classes of organized matter at a nanoscale. Evaporation drives self-organization of nanoparticles, nanorods, and nanotubes into nanoarchitectural structures whose construction is governed by capillary forces,<sup>1</sup> entropy, and chemistry of the nanobricks. Evaporation induced self-assembly is also on the ground of construction of mesoporous organized materials; evaporation drives the formation and organization of micelles that act as templates of mesopores.<sup>2</sup> The final topology and organization of the pores is governed by the dimension and mesostructural order of the micelles; removal of the template leaves an ordered porous structure. A step ahead to the construction of complex materials is achieving hierarchical porosity, with the possibility to integrate different functions at the different length scales of the pores.<sup>3</sup> Building hierarchical nanoporous materials through self-assembly is a nice challenge for materials science; we can even image self-organization of templating objects of different nanodimensions and shapes that can produce multiscale porous ordered materials.

Several strategies to fabricate hierarchical porous materials through self-assembly can be envisaged; they

basically rely on the capability of using templates of different dimensions which are able to organize during solvent evaporation. Easy removal of the template at the end of the process and interconnectivity between small and bigger pores are also important requirements to be fulfilled.<sup>4</sup> To build up hierarchical nanoporous materials we therefore have to control pore dimension, pore organization, and if possible pore shape; if we employ different types of templates another important requirement is the possibility of achieving a selective templating removal. Taking in mind these strict requirements, we have developed an alternative route to hierarchical nanoporous films through evaporation induced self-assembly (EISA).

The choice of the second template to produce a hierarchical material is dictated by the limitation that it should not interfere with the self-assembly process and should allow a pore dimension and shape control, if possible. Most of the strategies that have been proposed so far to produce hierarchical porous materials are restricted to the introduction of nano-objects of well-defined shape and their removal after self-organization.<sup>5</sup> It has been demonstrated that it is possible to use organic polymer nanospheres that remain in the film without disrupting organization during EISA and removing them by thermal calcination.<sup>6</sup> This approach is limited by the fact that one template, the micelles, self-organizes and

\*To whom correspondence should be addressed. E-mail: plinio@uniss.it.

- (1) Cui, Y.; Bjork, M. T.; Liddle, J. A.; Sonnichsen, C.; Boussett, B.; Alivisatos, A. P. *Nano Lett.* **2004**, *4*, 1093.
- (2) (a) Brinker, C. J.; Lu, Y.; Sellinger, A.; Fan, H. *Adv. Mater.* **1999**, *11*, 579. (b) Grosso, D.; Cagnol, F.; Soler-Illia, G.; Crepaldi, E. L.; Amenitsch, H.; Brunet-Brunau, A.; Bourgeois, A.; Sanchez, C. *Adv. Funct. Mater.* **2004**, *14*, 309. (c) Antonietti, M.; Ozin, G. A. *Chem.—Eur. J.* **2004**, *10*, 28. (d) Soler-Illia, G.; Innocenzi, P. *Chem.—Eur. J.* **2006**, *12*, 4478.
- (3) See, e.g., Jaroniec, M.; Schuth, F. *Chem. Mater.* **2008**, *20*, 599 (Preface to the Special Issue: Templated Materials).

- (4) Kuang, D.; Brezesinski, T.; Smarsly, B. *J. Am. Chem. Soc.* **2004**, *126*, 10534.
- (5) (a) Sel, O.; Kuang, D.; Thommes, M.; Smarsly, B. *Langmuir* **2006**, *22*, 2311. (b) Sel, O.; Brandt, A.; Wallacher, D.; Thommes, M.; Smarsly, B. *Langmuir* **2007**, *23*, 4724.
- (6) Falcaro, P.; Malfatti, L.; Kidchob, T.; Giannini, G.; Falqui, A.; Casula, M. F.; Amenitsch, H.; Marmiroli, B.; Grecni, G.; Innocenzi, P. *Chem. Mater.* **2009**, *21*, 2055.

**Table 1.** Summary of the Films Prepared with the Different Salt Concentrations and the Phases That Have Been Observed

NaCl	Na <sub>2</sub> HPO <sub>4</sub>		
	32 mM	45.5 mM	54 mM
0.49 M	mesopores	mesopores	mesopores
0.7 M	mesopores	mesopores + nanoboxes	mesopores + nanoflakes
0.84 M	mesopores and salt precipitates on film surface	mesopores and salt precipitates on film surface	mesopores + nanoboxes

forms during EISA; the other one is added to the precursor sol and does not really participate to EISA, and its formation is not driven by solvent evaporation.

We have developed an alternative route that is based on forming a second template nanostructure during EISA that can be easily and selectively removed at the end of film processing. The idea is that the formation of salt nanocrystals acting as porogen materials can be driven by evaporation of the solvent. This approach has been previously used for generating porous materials, but the examples that have been reported are limited to particles<sup>7</sup> or bulk materials<sup>8</sup> and the control of pore shape and dimension could not be achieved. What we present is a general synthesis method for producing pores of well-defined shapes and hierarchical porous thin films.

### Experimental Section

A triblock copolymer surfactant, Pluronic F127, tetraethyloctosilicate (TEOS), methyltriethoxysilane (MTES), ethanol (EtOH), sodium chloride, NaCl, and sodium phosphate monoacid, Na<sub>2</sub>HPO<sub>4</sub>, have been purchased from Aldrich and used as received; (100) oriented, P-type/boron doped silicon wafers (Jocam) and silica glass slides have been used as substrates.

The precursor solution has been prepared in different steps: at first we have prepared a sol, following a well established protocol, for the preparation of MTES-TEOS hybrid mesoporous films.<sup>9</sup> The sol is prepared in two stages; in the first one a stock solution has been prepared by mixing 3.08 mL of EtOH, 2.84 mL of TEOS, 1.42 mL of MTES, and 0.355 mL of an acidic water solution (HCl  $7.68 \times 10^{-1}$  M); the solution has been stirred for 1 h at 25 °C in a closed vessel. In the second stage a solution containing the surfactant has been prepared by dissolving 1.3 g of Pluronic F127 in 15 mL of EtOH and 1.5 mL of acidic water (HCl  $5 \times 10^{-3}$  M). Finally the two solutions have been mixed together and stirred for 15 min at 25 °C in a closed vessel. The final molar ratios of the mixture were the following: TEOS:MTES:EtOH:H<sub>2</sub>O:HCl: F127 = 1:0.56:24.48:8.13:0.11:7.6  $\times 10^{-3}$ .

We then prepared a salt solution by dissolving NaCl and Na<sub>2</sub>HPO<sub>4</sub> in water at different relative concentrations, as shown in Table 1 (vide infra), and we have added this salt solution to the silica sol. In a typical preparation we have added 20 mL of the MTES-TEOS-Pluronic solution to 3.6 mL of mixed salt aqueous solution; the molar concentrations of NaCl and Na<sub>2</sub>HPO<sub>4</sub> in Table 1 are referenced to a solution of 23.6 mL. To compare

the effects induced by the salt solution, we have also prepared a sol containing only NaCl or Na<sub>2</sub>HPO<sub>4</sub> using the same recipe and molar ratios. Silicon substrates, previously cleaned with water and EtOH, have been dip-coated at a  $15 \text{ cm} \cdot \text{min}^{-1}$  withdrawal rate using a home-built dip-coating system; the temperature in the deposition room has been kept at 25 °C and the relative humidity (RH) at 25%. The films, immediately after their deposition, have been dried at 80 °C for 18 h in air, then at 150 °C for 2 h, and finally calcined in air at room pressure at 350 °C for 3 h. To remove the salt nanocrystals from the films, the samples have been immersed in water and sonicated for 5 min.

Fourier transform infrared (FTIR) analysis was performed using a Bruker Vertex 70 V spectrophotometer. The optical bench and the sample compartment were kept in a vacuum during the measurement at a pressure lower than 0.5 hPa. The measurements were done using a Globar source, a Si beamsplitter, and a RT-DTGS-FIR detector. The spectra were recorded in transmission, in the  $600\text{--}50 \text{ cm}^{-1}$  range by averaging 32 scans with  $4 \text{ cm}^{-1}$  of resolution. A silicon wafer was used as the substrate to measure the background; the baseline was calculated by a rubberband algorithm (OPUS 7 software) while no smoothing on the data was performed. X-ray diffraction (XRD) measurements were recorded by a Bruker D8 diffractometer equipped with a scintillator counter. The Cu K $\alpha$  radiation was used to perform an  $\omega/2\theta$  scan from 25 to 60° with a resolution of 0.02°.

Sample morphology was analyzed by transmission electron microscopy (TEM) using a JEOL 200CX microscope equipped with a tungsten cathode operating at 200 kV. Finely ground films scratched from the silicon substrate were deposited on a carbon-coated copper grid for TEM observations.

The mesostructure of the films was evaluated by two-dimensional grazing incidence small-angle X-ray scattering (GISAXS) at the Austrian SAXS beamline of ELETTRA synchrotron (Trieste, Italy). An incident energy of 8 keV (wavelength 1.54 Å) was used; the instrumental glancing angle between the incident radiation and the sample was set slightly above the critical angle (grazing incidence). A two-dimensional CCD detector (Photonics Science, U.K.) was used to acquire the scattering patterns; each measurement consisted typically on the average of 10 acquisitions with integration time ranging from 20 ms to 1 s.

The film thickness was measured by an  $\alpha$ -SE Wollam spectroscopic ellipsometer.

Atomic force microscopy (AFM) was performed on the surface of the films by a NT-MDT Ntegra AFM in noncontact mode.

### Results and Discussion

We have deposited hybrid organic–inorganic silica mesostructured films through EISA from a precursor sol containing methyltriethoxysilane (MTES) and tetraethoxysilane (TEOS) as the alkoxides. This sol allows preparing hybrid organic–inorganic films that exhibit a strong capability to form highly organized mesostructures using both ionic or block copolymer surfactants.<sup>9,10</sup> We have used a triblock copolymer (F127) as template which is easily removed upon calcination of the film in air

- (7) Kim, S. H.; Liu, B. Y. H.; Zachariah, M. R. *Langmuir* **2004**, *20*, 2523.  
 (8) Lu, A. H.; Li, W. C.; Schmidt, W.; Schüth, F. *Microporous Mesoporous Mater.* **2006**, *95*, 187.  
 (9) Falcaro, P.; Costacurta, S.; Mattei, G.; Amenitsch, H.; Marcelli, A.; Cestelli Guidi, M.; Piccinini, M.; Nucara, A.; Malfatti, L.; Kidchob, T.; Innocenzi, P. *J. Am. Chem. Soc.* **2005**, *127*, 3838.

- (10) (a) De Theije, F. K.; Balkenende, A. R.; Verheijen, M. A.; Baklanov, M. R.; Mogilnikov, K. P.; Furukawa, Y. *J. Phys. Chem. B* **2003**, *107*, 4280. (b) Balkenende, A. R.; de Theije, F. K.; Kriege, J. C. K. *Adv. Mater.* **2003**, *15*, 139.

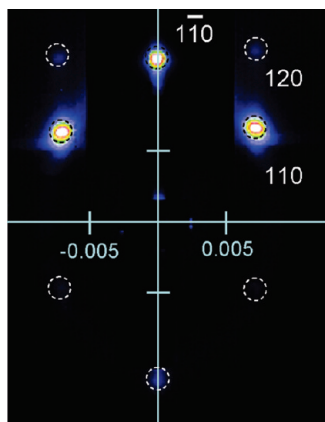


**Figure 1.** GI-SAXS pattern of a mesoporous hybrid thin film (sample 0.7 M NaCl–45.5 mM Na<sub>2</sub>HPO<sub>4</sub>) after thermal treatment at 350 °C. Indexation of the body centered cubic mesophase is shown in the figure.

at temperatures between 150 and 200 °C.<sup>11</sup> This temperature is low enough to maintain the covalently bonded methyl groups into the film without affecting the organization of the mesophase. The presence of the methyl groups is very important because they limit the absorption of water into the mesopores.<sup>12</sup>

After the addition of the aqueous salt solution of NaCl and Na<sub>2</sub>HPO<sub>4</sub>, the MTES-TEOS sol is becoming quickly transparent and the films appear optically homogeneous and transparent. We have prepared a set of different samples changing the relative salt concentrations as reported in Table 1. We have analyzed by SAXS the MTES-TEOS films that have been fired at 350 °C, and we have observed diffraction spots that have been attributed to the formation of an organized cubic mesophase. The patterns have been assigned to a cubic symmetry mesostructure (body centered cubic, *Im* $\bar{3}$ *m* in the space group) with the (110) plane oriented perpendicular to the substrate (*z* direction), uniaxially distorted.<sup>13</sup> Following this attribution, the interplanar distances have been calculated (sample 0.7 M NaCl–45.5 mM Na<sub>2</sub>HPO<sub>4</sub>) to be  $d_{1-10} = 16.7 \pm 1.8$  nm and  $d_{110} = 13.7 \pm 2$  nm (Figure 1). All the samples observed have shown the formation of ordered mesopores (Table 1); clearly the addition into the precursor sol of the salts does not interfere with the EISA process during the film deposition. The images taken by transmission electron microscopy (sample 0.7 M NaCl–45.5 mM Na<sub>2</sub>HPO<sub>4</sub>) have revealed, however, the presence of different types of nanoscale structures that appear spherical and cubic (Figure 2). The thermal calcination has removed the templating organic micelle formed by the block copolymer and has left a porous organized structure with mesopores of spherical appearance and dimensions of  $6.3 \pm 0.6$  nm; they are well

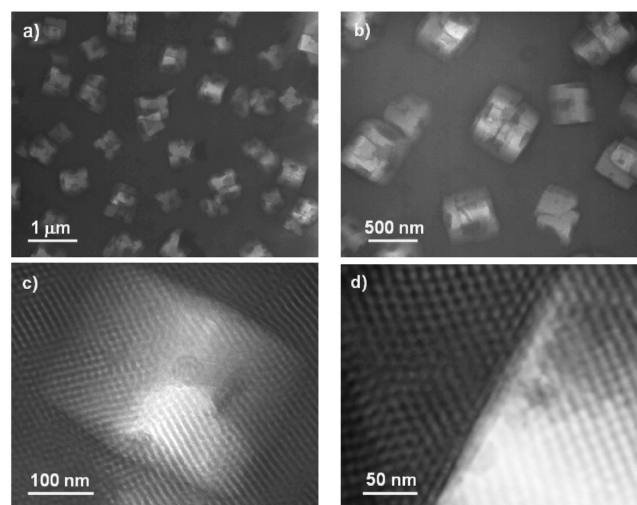


**Figure 2.** TEM images (a-d) at different magnifications of the film (sample 0.7 M NaCl–45.5 mM Na<sub>2</sub>HPO<sub>4</sub>) showing the presence of mesopores and nanoboxes.

organized into a cubic structure by EISA during film deposition. At the same time the salts added in the precursor solutions have allowed forming another type of nanostructure which appears as a cubic box of larger dimensions, typically in the range of 100–280 nm. The cubic salt nanoboxes can be easily removed by washing the film by water; the salt crystals are water-soluble, and after removal they leave empty pores. It is important to stress that the overall process does not disrupt the mesophase; the ordered porous phase maintains its arrangement after thermal treatment at 350 °C and the following washing process. The typical film thickness after the thermal treatment, evaluated by spectroscopic ellipsometry, is around 400 nm. The evaporation of the ethanol and water during EISA drives self-organization of the templating micelles and also induces precipitation of cubic salt nanocrystals. It should be underlined that obtaining NaCl nanocrystals in films by EISA is a very difficult task because evaporation of the solvent is very fast and the presence of ethanol together with the high acidic conditions in the precursor sol could cause immediate salt crystallization. We could not obtain nanoboxes using only NaCl or Na<sub>2</sub>HPO<sub>4</sub> as templating agent, even if we systematically changed the composition of the sol and the salt concentration. The role of Na<sub>2</sub>HPO<sub>4</sub> appears critical in avoiding the precipitation of NaCl and seeding the crystal formation. On the other hand the crystallized salt shows a well-defined shape and dimension which is an indication that the overall process is controlled. We can observe that only some specific compositions allow forming NaCl nanocrystals (Table 1), while in one case (sample 0.7 M NaCl–54 mM Na<sub>2</sub>HPO<sub>4</sub>) a very peculiar “flake-like” nanostructure is observed. In other samples the formation of white salt precipitates on the film surface is observed (samples 0.84 M NaCl–32 mM Na<sub>2</sub>HPO<sub>4</sub> and 0.84 M NaCl–45.5 mM Na<sub>2</sub>HPO<sub>4</sub>). The TEM images of the films containing the salt nanocrystals are shown in Figure 3. The images of the 0.7 M NaCl–54 mM Na<sub>2</sub>HPO<sub>4</sub> film show the presence of piled symmetrical salt nanoboxes

- (11) Falcaro, P.; Grosso, D.; Amenitsch, H.; Innocenzi, P. *J. Phys. Chem. B* **2004**, *108*, 10942.
- (12) Malfatti, L.; Kidchob, T.; Falcaro, P.; Costacurta, S.; Piccinini, M.; Cestelli Guidi, M.; Marcelli, A.; Corrias, A.; Casula, M.; Amenitsch, H.; Innocenzi, P. *Microporous Mesoporous Mater.* **2007**, *103*, 113.
- (13) Innocenzi, P.; Malfatti, L.; Kidchob, T.; Falcaro, P.; Costacurta, S.; Guglielmi, M.; Mattei, G.; Amenitsch, H. *J. Synch. Rad.* **2005**, *12*, 734.



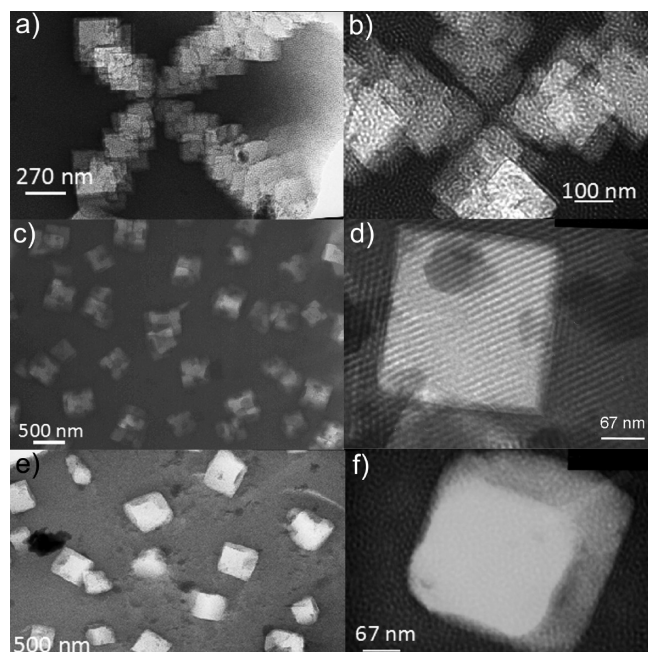


**Figure 3.** TEM images (a–f) at different magnifications of the films: (a, b) sample 0.7 M NaCl–54 mM Na<sub>2</sub>HPO<sub>4</sub>; (c, d) sample 0.7 M NaCl–45.5 mM Na<sub>2</sub>HPO<sub>4</sub>; (e, f) sample 0.84 M NaCl–54 mM Na<sub>2</sub>HPO<sub>4</sub>.

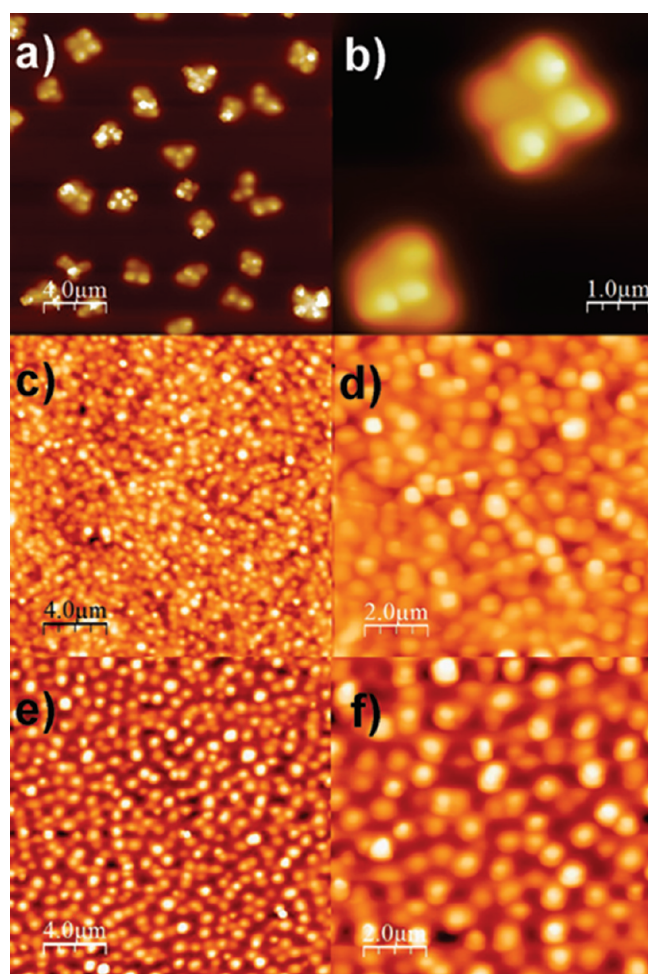


**Figure 4.** AFM images (a–f) at different magnifications of the films: (a, b) sample 0.7 M NaCl–54 mM Na<sub>2</sub>HPO<sub>4</sub>; (c, d) sample 0.7 M NaCl–45.5 mM Na<sub>2</sub>HPO<sub>4</sub>; (e, f) sample 0.84 M NaCl–54 mM Na<sub>2</sub>HPO<sub>4</sub>.

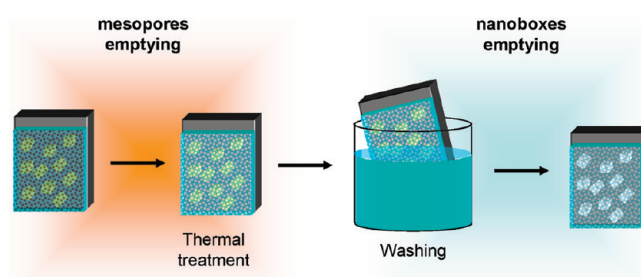


**Figure 5.** Illustration of the different steps to prepare hierarchical porous films with mesopores (2–10 nm) and cubic pores (50–400 nm).

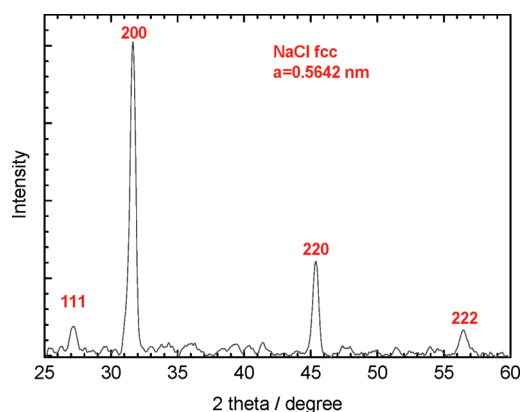


**Figure 6.** XRD pattern of a mesoporous film containing the salt nanocrystals; the indexation of the crystalline phase is shown (sample 0.7 M NaCl–45.5 mM Na<sub>2</sub>HPO<sub>4</sub>).

of around 100 nm which form a structure that we have called “flake-like” (Figure 3a,b). The AFM film images of the surface (Figure 4a,b) reveal that this peculiar structure forms a very specific pattern also on the surface, where flower-like nanostructures, which are due to the piled nanoboxes within the film, are observed. On the other hand, beside this particular pattern we observed that the film surface shows a homogeneous distribution of nano-grains that we correlate to the formation of the salt nanoboxes within the films. It is important to observe that the film homogeneously covers these structures that do not form, even after salt washing out, on the film surface. Figure 3c–f shows the TEM images of the films 0.7 M NaCl–45.5 mM Na<sub>2</sub>HPO<sub>4</sub> and 0.84 M NaCl–54 mM Na<sub>2</sub>HPO<sub>4</sub>; the surface of these films is shown in Figure 4c–f. The nanoboxes formed in the 0.7 M NaCl–45.5 mM Na<sub>2</sub>HPO<sub>4</sub> film are bigger with respect to the sample prepared at a lower salt concentration. This process appears simple and highly reproducible; we have, in fact, repeated several times the preparation, always obtaining similar results. The formation of salt nanocrystals gives pores of well-defined shape, while a certain control of pore dimension and topological distribution can be achieved by changing the salt concentration and relative salt composition.

The production process of the hierarchical material is illustrated in Figure 5: in the first step a mesostructured film is produced by EISA and the film contains mesopores and salt nanoboxes; in the second step the film is fired in air at 350 °C to remove the block copolymer template, the mesopores are now empty, and the nanoboxes

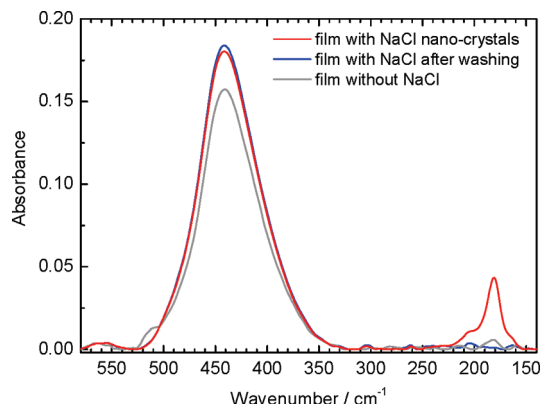


**Figure 7.** Far-infrared spectrum in the 580–140  $\text{cm}^{-1}$  range of films at different steps of preparation (sample 0.7 M NaCl–45.5 mM  $\text{Na}_2\text{HPO}_4$ ).

are still filled. In the final step the film is washed by water and then dried; this process allows eliminating the salt, leaving empty nanoboxes. The advantage of this procedure is given by the selective control of nanopore formation through film processing and that the templates, which are organic micelles and salt nanocrystals, are formed in their final shape during EISA. The nanoboxes are not ordered but result as homogeneously dispersed within the mesoporous matrix. We have used X-ray diffraction (XRD) (Figure 6) and far-infrared (FIR) spectroscopy (Figure 7) to identify the nanocrystalline templating phase that is formed by EISA, both the data show that it is crystalline sodium chloride (sample 0.7 M NaCl–45.5 mM  $\text{Na}_2\text{HPO}_4$ ). The XRD pattern in

the 25–60° range shows four sharp diffraction peaks, 111, 200, 220, and 222, which represent the typical signature of crystalline sodium chloride; the XRD patterns of the sample without the salt and after washing show only the background noise. The FIR spectra show an intense absorption band at 440  $\text{cm}^{-1}$  which is assigned to the silica rocking mode and another band at 170  $\text{cm}^{-1}$  due to phononic modes in crystalline NaCl. The spectra show that the washing process completely removes the salt within the film and is able, therefore, to leave empty nanoboxes.

## Conclusions

We have developed a new synthesis route that allows the formation of two types of pore templates during EISA, spherical micelles from block copolymers and crystalline nanoboxes from salts. Formation of NaCl nanocrystals is driven by the evaporation of the solvent during film deposition while uncontrolled precipitation of the salt is avoided by the coaddition of  $\text{Na}_2\text{HPO}_4$  in the precursor sol. The removal of the template can be done in a selective way; block copolymers are eliminated by thermal treatment and salt nanoboxes are removed by a simple water washing of the film. The final material appears as a porous hierarchical film with two ranges of porosities, an ordered array of mesopores, and cubic nanoboxes of around 260 nm from the salt nanocrystals. This method will allow a selective functionalization of the nanopores through a controlled multistep process.